Research Square

Preprints are preliminary reports that have not undergone peer review.
They should not be considered conclusive, used to inform clinical practice,
or referenced by the media as validated information.

Scenario-Based Assessment of Thermal Performance, Battery Degradation, and Total Cost of Ownership for EV Battery Thermal Management in Tropical Logistics Operations

Praphat Phuangchuen
Institute of Vocational Education Eastern Region, Thailand
Thunyaput Kittiphotiklang
Institute of Vocational Education Eastern Region, Thailand
Siriwat Ninlawat
Nakhon Phanom University
Wirasak Chotikandun
wirasak@techsakon.ac.th

Sakon Nakhon Technical College,
Prakasit Prabpal
Udon Thani Technical College
Somchat Sonasang
Nakhon Phanom University

Research Article

Keywords:

Posted Date: October 30th, 2026

DOI: https://doi.org/10.21203/rs.3.rs-11382515/v1

License: This work is licensed under a Creative Commons Attribution 4.0 International License.
Read Full License

Additional Declarations: No competing interests reported.

Scenario-Based Assessment of Thermal Performance, Battery Degradation, and Total Cost of Ownership for EV Battery Thermal Management in Tropical Logistics Operations

Praphat Phuangchuen[1], Thunyaput Kittiphotiklang[2], Siriwat Ninlawat[3], Wirasak Chotikandun[4*], Prakasit Prabpal[5], Somchat Sonasang[6]

[1] Department of Mechanical Technology, Institute of Vocational Education Eastern Region, Rayong, 21000, Thailand .
[2] Department of Electrical Technology, Institute of Vocational Education Eastern Region, Rayong, 21000, Thailand .
[3] Department of Electrical Technology, Faculty of Industrial Technology, Nakhon Phanom University, Nakhon Phanom, 48000, Thailand .
[4*] Department of Mechanical Technology, Sakon Nakhon Technical College, Institute of Vocational Education Northeastern Region 2, Sakon Nakhon, 47000, Thailand .
[5] Department of Electrical Technology, Udon Thani Technical College, Institute of Vocational Education Northeastern Region 1, Udon Thani, 41000, Thailand .
[6] Electrical Elements and Wireless Devices Unit, Faculty of Industrial Technology, Nakhon Phanom University, Nakhon Phanom, 48000, Thailand .

*Corresponding author(s). E-mail(s): wirasak@techsakon.ac.th;
Contributing authors: praphat.p@technicrayong.ac.th; thunyaput.k@technicrayong.ac.th; siriwut.n@npu.ac.th; prakasit.pra@udontech.ac.th; somchat.s@npu.ac.th;

Abstract

Battery thermal management affects electric-vehicle (EV) battery service life, replacement frequency, lifecycle cost, and the timing of battery entry into end-of-life (EOL) management systems. This study develops a deterministic scenario-based framework for tropical logistics operation by linking prescribed battery-temperature trajectories, state-of-health (SoH) decline, replacement events, and an eight-year total cost of ownership (TCO) model. Passive air cooling, reactive liquid cooling, and predictive pre-cooling are compared under a 28–38 °C tropical peak-day profile. The respective peak battery temperatures are 51.07, 33.41, and 31.00 °C, while first-pack 80%-SoH crossing times are 3.43, 5.87, and 10.14 years. Over eight years, the three strategies produce two, one, and zero battery-replacement events, respectively. The resulting TCO values are USD 77,700, USD 72,500, and USD 62,000 per vehicle, giving predictive pre-cooling a 20.21% saving relative to passive air cooling. Predictive pre-cooling also defers two traction-battery EOL entries per vehicle beyond the study horizon. The results indicate that improved thermal management can extend battery service life, reduce replacement-related cost, and slow battery material turnover, although the numerical results remain scenario-based and require experimental validation.

Keywords: battery thermal management, battery service life, end-of-life battery, total cost of ownership, tropical logistics

1 Introduction

The rapid growth of electric mobility is increasing not only the demand for lithium-ion batteries but also the future volume of traction batteries entering end-of-life management systems. Electric-vehicle (EV) batteries contain energy- and resource-intensive materials, and premature retirement increases the demand for replacement packs while accelerating the flow of spent batteries toward reuse, repurposing, disassembly, and recycling pathways. From a material-cycle perspective, extending the useful service life of an EV battery is therefore an upstream resource-efficiency and waste-prevention strategy that complements downstream recycling. Waste-prevention research has long emphasized reduction and reuse as high-priority measures in sustainable resource management, while end-of-life vehicle studies have highlighted the need to integrate operational, economic, and material-flow considerations throughout the vehicle life cycle [1, 2]. Recent work on EV battery recycling similarly shows that battery lifetime, second-life utilization, disassembly, and material recovery are closely linked elements of a circular battery system [3, 4].

Among the operational factors that determine battery service life, temperature is particularly important. Lithium-ion battery performance, safety, efficiency, and degradation rate are strongly influenced by both the magnitude and duration of thermal exposure. Classical electrochemical energy-balance formulations identify irreversible ohmic and reaction heat together with reversible entropic heat as the principal mechanisms governing battery heat generation [5]. At the vehicle level, battery thermal

management systems (BTMSs) are therefore required to maintain battery temperature within an acceptable operating range, limit excessive temperature gradients, and reduce thermal stress. Available BTMS technologies include air cooling, liquid cooling, phase-change materials, direct refrigerant cooling, thermoelectric systems, and hybrid configurations [6–11]. No single architecture is universally superior because improved thermal control is normally obtained at the expense of additional hardware, auxiliary power, mass, control complexity, and maintenance requirements.

This trade-off becomes particularly important under tropical operating conditions. Elevated ambient temperature reduces the available temperature difference for passive heat rejection and can increase both the duration and severity of battery thermal exposure. Long-term ageing studies have shown that temperature interacts with state of charge, cycling history, and current rate to accelerate capacity fade and internal-resistance growth [12, 13]. Vehicle-level studies under realistic operating profiles further indicate that climatic conditions and driving schedules can materially change battery ageing and thermal-management demand [14, 15]. Elevated ambient temperature can also increase vehicle-level energy demand and reduce driving range because a larger fraction of the available energy must be allocated to thermal conditioning and associated auxiliary loads [16]. Recent evidence from tropical and high-temperature operating environments reinforces this concern, showing that hot ambient conditions can expose EV batteries to substantially higher thermal stress and can increase degradation risk, particularly when combined with intensive charging and vehicle utilization [17, 18]. For commercial logistics fleets, where vehicles may follow repeated daily routes with high utilization and limited recovery periods, these effects can accumulate over several years of operation.

Conventional thermal-control strategies generally respond after battery temperature approaches a predefined threshold. Predictive approaches instead use information about expected driving demand, charging events, ambient conditions, or future thermal states to initiate cooling before critical conditions occur. Nonlinear model-predictive control and integrated vehicle thermal-management studies have demonstrated the potential to coordinate battery temperature and auxiliary-energy consumption more effectively than purely reactive control [19, 20]. More recent work has incorporated vehicle-speed information, battery degradation objectives, and coordinated driving–charging conditions into predictive thermal-management formulations [21–23]. From a battery-life perspective, the potential benefit of predictive control is not limited to reducing instantaneous peak temperature; reducing cumulative thermal exposure can also delay degradation and, consequently, postpone the point at which a traction battery reaches its end-of-life criterion.

The material-cycle implication of such life extension is important. Most circular-economy research on EV batteries has understandably concentrated on downstream stages, including collection, second-life use, disassembly, recycling technology, material recovery, and recycling-system efficiency [3, 4]. These processes are essential because spent batteries contain valuable materials that should remain within productive material cycles rather than be lost as unmanaged waste. However, the timing at which batteries enter these downstream systems is itself influenced by decisions made during the use phase. A thermal-management strategy that extends traction-battery

service life can reduce the frequency of replacement over a fixed vehicle operating horizon and thereby defer the generation of end-of-life battery packs. This does not eliminate the eventual need for reuse or recycling, but it can improve resource productivity by extracting a longer useful service period from the same battery asset before downstream treatment becomes necessary.

The economic consequences of this relationship are equally important. Advanced BTMS architectures generally require higher initial investment and may consume more auxiliary energy than passive cooling systems. These additional costs must be balanced against potential reductions in degradation, battery replacement, maintenance, and vehicle downtime. Techno-economic reviews of EV thermal-management technologies have emphasized that thermal performance alone is insufficient for selecting a preferred BTMS because lifecycle cost depends on the interaction between capital expenditure, operating energy, component durability, and battery lifetime [24]. Degradation-aware economic studies have likewise demonstrated the value of incorporating battery ageing into operational decision making [25]. In Thailand and similar emerging EV markets, total-cost-of-ownership analyses further show that energy prices, maintenance costs, battery-related expenditure, utilization intensity, and local operating conditions can substantially affect EV economics [26]. For high-mileage logistics fleets, avoided or deferred battery replacement can therefore represent both an economic benefit and an upstream material-efficiency benefit.

Despite these advances, an important gap remains between battery thermal-management studies and material-cycle decision support. High-fidelity electrothermal and control studies typically focus on temperature regulation, energy consumption, or degradation minimization, whereas end-of-life battery studies generally begin after the battery has already reached retirement. Comparatively little attention has been given to transparent use-phase screening frameworks that trace how alternative thermal-management strategies may propagate from daily thermal exposure to long-term state-of-health (SoH), battery-replacement timing, ownership cost, and the timing of end-of-life battery generation. This gap is particularly relevant for tropical logistics applications, where repeated high-temperature operation may accelerate the transition from useful battery service to replacement and downstream waste-management stages.

The present study addresses this gap through a deterministic scenario-based assessment of three EV battery thermal-management strategies—passive air cooling, reactive liquid cooling, and predictive pre-cooling—under a common tropical logistics operating framework. The objective is not to reproduce cell-level electrochemistry or to claim a trained machine-learning controller. Instead, the study provides a transparent screening model in which prescribed thermal trajectories are propagated through battery SoH, replacement timing, and eight-year total cost of ownership (TCO). The work makes four main contributions. First, it quantifies the thermal exposure associated with three contrasting BTMS strategies under a tropical peak-day condition. Second, it links these thermal scenarios to long-term SoH decline and identifies when the assumed 80% end-of-life threshold is reached. Third, it connects battery-replacement timing with capital cost, auxiliary-energy use, maintenance, downtime, and cumulative TCO in a consistent lifecycle-economic framework. Finally, it interprets avoided or deferred

battery replacement as an upstream indicator of battery-life extension and delayed entry into the end-of-life management chain, thereby connecting operational thermal management with broader material-cycle and waste-prevention considerations. Sensitivity analyses for ambient temperature, electricity tariff, pre-cooling duration, and fleet size are additionally used to identify the operating conditions under which proactive thermal management provides the greatest lifecycle benefit.

2 Methodology

2.1 Study Framework, System Boundary, and Thermal-Management Strategies

This study develops a deterministic scenario-based framework for evaluating how alternative electric-vehicle battery thermal-management strategies may influence thermal exposure, battery service life, replacement frequency, end-of-life (EOL) entry, and lifecycle ownership cost under tropical logistics operation. The analytical chain is structured as

$$\text{BTMS strategy} \rightarrow T_s(h) \rightarrow \mathrm{SoH}_s(y) \rightarrow y_{\mathrm{EOL},s} \rightarrow N_{\mathrm{rep},s} \rightarrow C_{\mathrm{TCO},s}, \tag{1}$$

where s denotes the thermal-management strategy, $T_s(h)$ is the prescribed daily battery-temperature trajectory, $\mathrm{SoH}_s(y)$ is the corresponding long-term state-of-health trajectory, $y_{\mathrm{EOL},s}$ is the first EOL threshold-crossing time, $N_{\mathrm{rep},s}$ is the number of battery-replacement events during the ownership horizon, and $C_{\mathrm{TCO},s}$ is the resulting total cost of ownership. The overall analytical framework is illustrated in Fig. 1. The framework separates the thermal, degradation, material-cycle, and economic layers while preserving the information flow among them. The selected BTMS strategy defines the prescribed thermal exposure, which is associated with a strategy-specific degradation trajectory and traction-battery end-of-life timing. The resulting replacement events subsequently affect both the number of battery packs entering the end-of-life management chain and the cumulative ownership cost. This structure allows the consequences of thermal-management decisions to be interpreted from operational, economic, and resource-efficiency perspectives.

The overall analytical framework is illustrated in Fig. 1. The framework explicitly separates the thermal, degradation, material-cycle, and economic layers while preserving the information flow between them. Thermal-management strategy determines the prescribed thermal exposure; the paired degradation model determines battery service life and traction end-of-life timing; replacement events then affect both the number of battery packs entering the end-of-life management chain and the cumulative ownership cost. This structure enables thermal-management decisions to be interpreted simultaneously from operational, economic, and resource-efficiency perspectives.

The system boundary extends from vehicle operation through traction-battery retirement. Downstream second-life processing, disassembly, hydrometallurgical or pyrometallurgical recycling, and recovered-material yields are not explicitly simulated. Instead, the number and timing of battery packs reaching the assumed traction EOL criterion are used as upstream material-cycle indicators. This interpretation is

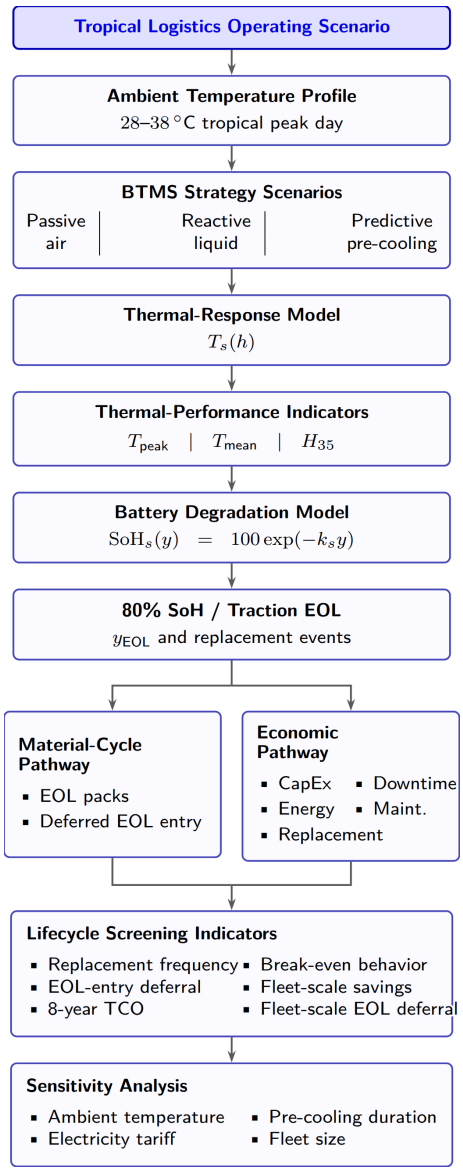


Fig. 1 Proposed scenario-based framework linking BTMS strategy, battery degradation, end-of-life timing, and lifecycle cost.

consistent with the principle that extending product service life can delay material throughput and complement downstream recovery and recycling activities [1, 3, 4].

Three BTMS strategies are compared over an eight-year ownership horizon: passive air cooling, reactive liquid cooling, and predictive pre-cooling. All strategies are evaluated using the same tropical ambient-temperature profile, traction-energy requirement, economic horizon, and vehicle utilization assumptions. Consequently,

differences among cases arise from the prescribed thermal behavior, BTMS auxiliary-energy demand, degradation trajectory, replacement requirement, maintenance burden, downtime, and initial thermal-management investment.

The framework is intentionally formulated as an engineering screening model rather than a high-fidelity battery simulation. The temperature trajectories are analytical surrogate functions chosen to represent qualitatively distinct thermal-management behaviors. They are not outputs of a cell-resolved electrochemical model, computational-fluid-dynamics calculation, experimentally calibrated reduced-order thermal model, or trained machine-learning predictor. The resulting numerical values should therefore be interpreted as internally consistent comparative scenario outputs rather than experimentally validated predictions.

2.2 Tropical Ambient and Battery-Temperature Scenarios

The tropical peak-day ambient-temperature profile is represented as

$$T_{\mathrm{amb}}(h) = \mathrm{clip}\left[28 + 10\sin\left(\frac{\pi(h-6)}{12}\right), 28, 38\right], \tag{2}$$

where h denotes the hour of day. The clipping operator imposes a nighttime lower bound of 28 °C and a daytime maximum of 38 °C, thereby providing a simplified high-temperature operating environment representative of the screening conditions considered in this study.

The passive-air case is described by

$$T_{\mathrm{pass}}(h) = T_{\mathrm{amb}}(h) + 8 + 6\exp\left[-\frac{(h-14)^2}{8}\right]. \tag{3}$$

The constant 8 °C temperature rise represents persistent battery-to-ambient thermal elevation under limited heat rejection, while the Gaussian component represents an additional afternoon thermal load centered around 14:00. The formulation intentionally produces the most thermally stressed condition among the three strategies.

For reactive liquid cooling, the battery-temperature trajectory is represented using a bounded logistic response,

$$T_{\mathrm{react}}(h) = 30 + 4\,\sigma(h-11)\sigma(16-h), \tag{4}$$

with

$$\sigma(x) = \frac{1}{1+\exp(-x)}. \tag{5}$$

The two logistic terms form a smooth daytime activation window. The resulting trajectory represents a controller that reacts to increasing thermal load and maintains the battery within a substantially narrower temperature band than passive cooling.

The predictive pre-cooling case is expressed as

$$T_{\mathrm{pred}}(h) = 29.5 + 1.5\sin\left(\frac{\pi h}{12}\right) - 1.2\exp\left[-\frac{(h-11.5)^2}{0.5}\right]. \tag{6}$$

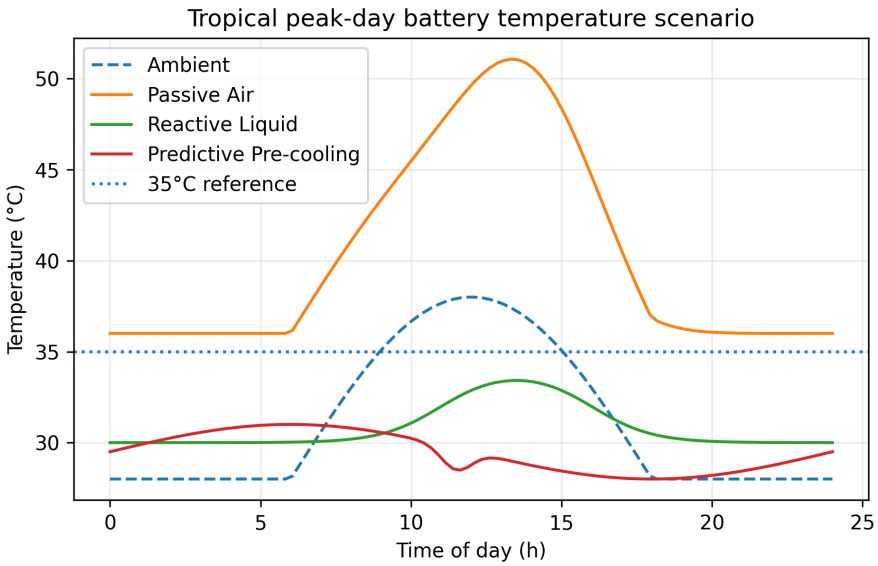


Fig. 2 Prescribed tropical peak-day ambient and battery-temperature trajectories for the three BTMS strategies. The 35 °C line is used as an engineering reference rather than a hard operating constraint.

The final negative Gaussian term represents cooling initiated before the expected high-load period. Accordingly, the trajectory is interpreted as a predictive pre-cooling scenario rather than a machine-learning prediction. No trained learning model is used or claimed in the present study.

The analytical forms in Eqs. (2)–(6) are deliberately retained in explicit form so that the source of each thermal feature can be traced. This transparency is important because the objective of the study is comparative lifecycle screening rather than reconstruction of detailed electrochemical heat generation. Physically based battery energy balances provide the underlying motivation for thermal management, since irreversible and reversible heat-generation processes ultimately determine cell temperature [5]; however, those processes are not individually resolved in the present surrogate model.

Three common thermal indicators are calculated for each strategy:

$$T_{\mathrm{peak},s} = \max_{0\le h\le 24} T_s(h), \tag{7}$$

$$\overline{T}_s = \frac{1}{24}\int_0^{24} T_s(h)\,dh, \tag{8}$$

$$H_{35,s} = \int_0^{24} \mathbb{I}[T_s(h) > 35]\;dh, \tag{9}$$

where $\mathbb{I}[\cdot]$ is an indicator function. These metrics distinguish peak thermal severity, average daily exposure, and exposure duration above the 35 °C engineering reference.

2.3 Battery Degradation, Service Life, and End-of-Life Entry

Battery degradation is represented using a strategy-specific exponential screening relationship,

$$\mathrm{SoH}_s(y) = 100 \exp(-k_s y), \tag{10}$$

where y is the battery operating age in years and k_s is the assumed degradation coefficient. The coefficients used in the three scenarios are

$$k_{\mathrm{pass}} = 0.065, \qquad k_{\mathrm{react}} = 0.038, \qquad k_{\mathrm{pred}} = 0.022 \quad \mathrm{yr}^{-1}. \tag{11}$$

The corresponding one-year SoH retention factors are 0.9371, 0.9627, and 0.9782, respectively. These values represent paired scenario assumptions rather than coefficients directly fitted to Eqs. (3)–(6). This distinction prevents an unsupported claim of direct temperature-to-degradation causality. Temperature, state of charge, cycling history, current rate, and calendar time are known to interact in lithium-ion battery degradation [12–15]; a calibrated multi-stressor degradation law is therefore identified as a necessary extension for future work.

An 80% SoH threshold is adopted as the traction-battery EOL reference. The continuous time required for a battery under strategy s to reach this level follows directly from Eq. (10):

$$y_{\mathrm{EOL},s} = -\frac{\ln(0.80)}{k_s}. \tag{12}$$

The corresponding first threshold-crossing times are 3.43 years for passive air cooling, 5.87 years for reactive liquid cooling, and 10.14 years for predictive pre-cooling.

To express the service-life benefit relative to the passive baseline, the EOL deferral is defined as

$$\Delta y_{\mathrm{EOL},s} = y_{\mathrm{EOL},s} - y_{\mathrm{EOL,pass}}. \tag{13}$$

This metric quantifies how long entry of a representative traction battery into the EOL management chain is deferred relative to passive air cooling. It should not be interpreted as avoided recycling; the battery ultimately still requires appropriate second-life assessment or recycling after retirement.

For annual economic accounting, a battery that falls below the 80% threshold is replaced at the next annual accounting point and the replacement battery is reset to 100% SoH. Let

$$N_{\mathrm{EOL},s}(H) = \sum_{j=1}^{H} \mathbb{I}\left[\mathrm{SoH}_{s,j} < 80\%\right] \tag{14}$$

denote the number of traction-battery retirement events within an ownership horizon H, with the SoH clock reset following each replacement.

Under the eight-year accounting horizon used here, this produces two replacement events for passive air cooling, occurring in years 4 and 8; one event for reactive liquid cooling, occurring in year 6; and no replacement event for predictive pre-cooling.

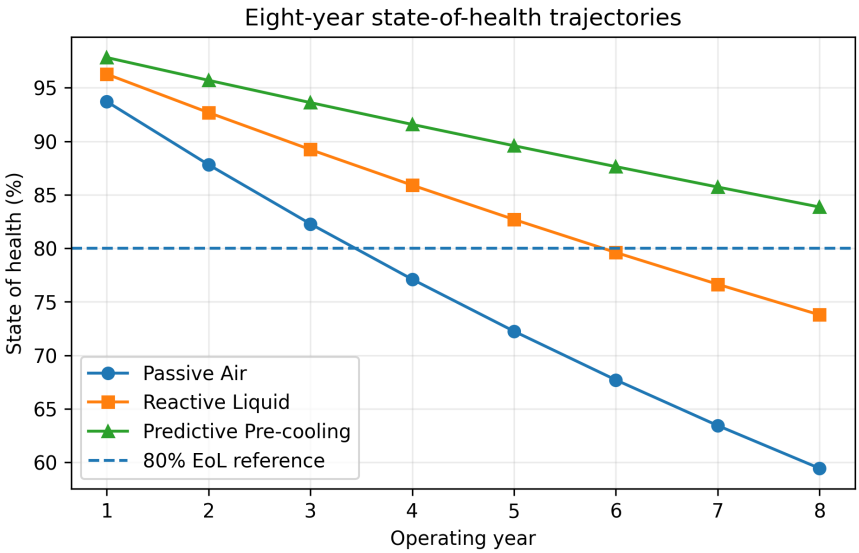


Fig. 3 Representative first-pack state-of-health trajectories used to determine service-life intervals. The 80% line indicates the assumed traction-battery end-of-life threshold. Replacement batteries are reset to 100% SoH in the annual ownership-cost accounting.

The avoided or deferred EOL-pack entries relative to the passive baseline are therefore represented by

$$A_{\mathrm{EOL},s}(H) = N_{\mathrm{EOL,pass}}(H) - N_{\mathrm{EOL},s}(H). \tag{15}$$

Equation (15) is an event-count indicator rather than a mass-based waste metric. Because battery mass, chemistry-specific material composition, second-life suitability, recycling yield, and recovered-material quality are outside the system boundary, the present study does not claim a quantitative reduction in waste mass or environmental impact.

2.4 Total Cost of Ownership and Replacement Accounting

The economic assessment follows a total-cost-of-ownership framework in which thermal-management investment is evaluated together with traction energy, BTMS auxiliary energy, battery replacement, downtime, and maintenance. Such lifecycle accounting is particularly relevant when a higher-cost thermal-management system may reduce degradation-related expenditure over the ownership period [24–26].

For strategy s, the eight-year TCO is

$$C_{\mathrm{TCO},s} = C_{\mathrm{cap},s} + C_{\mathrm{trac},s} + C_{\mathrm{BTMS},s} + C_{\mathrm{rep},s} + C_{\mathrm{down},s} + C_{\mathrm{maint},s}, \tag{16}$$

where C_{cap} is the initial BTMS and associated hardware cost, C_{trac} is traction-energy expenditure, C_{BTMS} is auxiliary thermal-management energy expenditure, C_{rep} is battery-replacement expenditure, C_{down} represents thermal- and maintenance-related vehicle downtime, and C_{maint} is the remaining maintenance cost.

Table 1 Eight-year cost and replacement inputs per vehicle used in the scenario model.

Component	Passive air	Reactive liquid	Predictive pre-cooling
Capital hardware (USD)	12,000	15,500	17,200
Traction energy (USD)	38,000	38,000	38,000
BTMS parasitic energy (USD)	1,200	4,100	3,200
Replacement events	2	1	0
Battery replacement (USD)	18,000	9,000	0
Downtime losses (USD)	6,500	2,400	800
Maintenance (USD)	2,000	3,500	2,800
Total TCO (USD)	77,700	72,500	62,000

A common battery-replacement event cost of USD 9,000 is used in the scenario model. Consequently,

$$C_{\mathrm{rep},s} = 9000\, N_{\mathrm{EOL},s}(8). \tag{17}$$

The resulting replacement expenditures are USD 18,000 for passive air cooling, USD 9,000 for reactive liquid cooling, and zero for predictive pre-cooling during the eight-year horizon. This event-based formulation makes the degradation, material-cycle, and economic layers internally consistent.

The absolute cost saving relative to passive air cooling is

$$\Delta C_s = C_{\mathrm{TCO,pass}} - C_{\mathrm{TCO},s}, \tag{18}$$

and the percentage saving is

$$S_s = 100 \frac{\Delta C_s}{C_{\mathrm{TCO,pass}}}. \tag{19}$$

A positive S_s therefore indicates that the alternative BTMS reduces eight-year ownership cost relative to passive air cooling.

For cumulative-cost analysis, traction energy, BTMS energy, downtime, and maintenance are distributed uniformly across the eight-year horizon, whereas battery replacement is treated as a discrete event. The cumulative cost at the end of year y is

$$C_{\mathrm{cum},s}(y) = C_{\mathrm{cap},s} + \frac{y}{8}\left(C_{\mathrm{trac},s} + C_{\mathrm{BTMS},s} + C_{\mathrm{down},s} + C_{\mathrm{maint},s}\right) + \sum_{j=1}^{y} C_{\mathrm{rep},s}(j). \tag{20}$$

For passive air cooling, replacement charges of USD 9,000 are introduced in years 4 and 8. For reactive liquid cooling, one USD 9,000 charge is introduced in year 6. No replacement charge is incurred by the predictive strategy within the eight-year horizon.

For comparison between passive air cooling and predictive pre-cooling,

$$D(y) = C_{\mathrm{cum,pass}}(y) - C_{\mathrm{cum,pred}}(y). \tag{21}$$

Before the first passive-battery replacement, the predictive strategy retains a higher cumulative cost because of its greater initial hardware expenditure. At year 3,

$$D(3) = -4112.5 \text{ USD}, \tag{22}$$

whereas after the first USD 9,000 replacement event,

$$D(4) = 5250 \text{ USD}. \tag{23}$$

Linear interpolation between the annual accounting points gives an indicative crossover of approximately

$$y_{\mathrm{BE}} = 3 + \frac{4112.5}{5250 + 4112.5} \approx 3.44 \text{ years}. \tag{24}$$

Because battery replacement is modeled as a discrete event, this value is best interpreted as an indicative graphical break-even rather than as a continuously accruing discounted payback period. In operational terms, the economic transition occurs during the first passive-battery replacement interval.

2.5 Sensitivity Analysis

The sensitivity analysis examines whether the comparative conclusions remain directionally stable when selected environmental and economic variables are changed. These relationships are screening functions and are not intended as empirically calibrated regressions.

The ambient-temperature sensitivity is represented by

$$C_{\mathrm{pass}}(T_a) = 5000 + 350(T_a - 28)^{1.5}, \tag{25}$$

$$C_{\mathrm{pred}}(T_a) = 6200 + 80(T_a - 28), \tag{26}$$

for

$$28 \leq T_a \leq 42 \ ^{\circ}\mathrm{C}. \tag{27}$$

The nonlinear passive relationship represents increasing economic exposure as thermal conditions become more severe, whereas the smaller predictive coefficient represents a strategy that is less sensitive to increasing ambient temperature. The numerical coefficients are scenario assumptions and should therefore be interpreted comparatively rather than as fitted fleet-cost parameters.

Electricity-tariff sensitivity is evaluated by scaling energy-related expenditure from the reference tariff of USD 0.12/kWh:

$$C_{\mathrm{energy},s}(p) = (C_{\mathrm{trac},s} + C_{\mathrm{BTMS},s}) \, \frac{p}{0.12}, \tag{28}$$

where p is the alternative electricity tariff. The calculation changes energy price only; electrical consumption, degradation coefficients, and replacement timing remain unchanged.

2.6 Predictive Pre-Cooling Screening

The influence of pre-cooling duration is represented using the first-order saturating relation

$$\Delta T_{\mathrm{peak}}(\tau) = 8.5\left(1 - e^{-\tau/15}\right), \tag{29}$$

where τ is the pre-cooling duration in minutes. The corresponding marginal temperature benefit is

$$\frac{d\Delta T_{\mathrm{peak}}}{d\tau} = \frac{8.5}{15} e^{-\tau/15}. \tag{30}$$

Equation (30) decreases monotonically with τ, explicitly representing diminishing thermal returns from increasingly long pre-cooling periods. This relationship is used only to explore the qualitative trade-off between intervention duration and peak-temperature mitigation; it is not presented as an experimentally identified cooling-system transfer function.

2.7 Fleet-Scale Economic and Material-Cycle Indicators

For a fleet containing N nominally identical vehicles, cumulative ownership-cost savings relative to passive cooling are

$$C_{\mathrm{fleet,sav},s}(N) = N\left(C_{\mathrm{TCO,pass}} - C_{\mathrm{TCO},s}\right). \tag{31}$$

For predictive pre-cooling, the present scenario gives a per-vehicle eight-year saving of

$$77{,}700 - 62{,}000 = 15{,}700 \text{ USD}. \tag{32}$$

The corresponding number of battery packs whose entry into the EOL management chain is deferred relative to the passive baseline is

$$N_{\mathrm{deferred},s} = N\left[N_{\mathrm{EOL,pass}}(8) - N_{\mathrm{EOL},s}(8)\right]. \tag{33}$$

For the present eight-year scenarios, reactive liquid cooling reduces the number of EOL entry events by one pack per vehicle relative to passive cooling, while predictive pre-cooling reduces it by two packs per vehicle.

The term "deferred" is used deliberately. Equation (33) does not represent avoided battery production, avoided waste mass, recycling yield, or environmental impact. Rather, it quantifies the timing effect of longer modeled battery service life on the number of traction-battery retirement events occurring within the fixed study horizon.

2.8 Computational Implementation and Reproducibility

All calculations are deterministic and implemented in Python. A common set of model parameters is used for the thermal, degradation, replacement, TCO, sensitivity, and fleet-scale calculations. The computational sequence is therefore internally traceable: the selected BTMS scenario determines the prescribed thermal trajectory; the paired

Table 2 Thermal indicators obtained for the prescribed tropical peak-day scenarios.

Strategy	T_{peak} (°C)	$\overline{T}$ (°C)	H_{35} (h/day)
Passive air	51.07	40.44	24.0
Reactive liquid	33.41	30.84	0.0
Predictive pre-cooling	31.00	29.44	0.0

degradation scenario determines the service-life interval; the service-life interval determines replacement timing and EOL-entry events; and these events are propagated into the economic and fleet-scale indicators.

No random sampling, stochastic degradation model, optimization algorithm, or trained learning model is used. Consequently, repeated calculations using the same parameter set produce identical results. The reproducibility claimed in this work refers to numerical reproducibility of the scenario analysis, not to predictive validation against field measurements.

The principal limitation of the methodology is that the thermal and degradation layers are coupled parametrically rather than through a calibrated electrothermal-aging model. Likewise, the material-cycle analysis tracks EOL pack-entry events rather than chemistry-specific material mass flows. These limitations are intentionally retained to provide a transparent first-stage screening framework. Future extensions should incorporate experimentally validated thermal parameters, temperature- and state-dependent ageing models, real logistics duty cycles, second-life eligibility, pack mass and chemistry, recycling yields, and discounted lifecycle cash flows.

3 Results and Discussion

3.1 Thermal Response and Battery Service-Life Implications

Figure 2 compares the prescribed tropical peak-day battery-temperature trajectories for the three thermal-management strategies. A clear separation is observed among the scenarios. Passive air cooling produces the highest peak battery temperature of 51.07 °C, whereas reactive liquid cooling limits the peak to 33.41 °C and predictive pre-cooling further reduces it to 31.00 °C. Relative to the passive-air scenario, the peak-temperature reductions are therefore 17.66 °C and 20.07 °C for reactive liquid cooling and predictive pre-cooling, respectively. These values correspond to reductions of 34.57% and 39.30%.

Peak temperature alone does not fully describe the thermal burden. The indicators defined in Eqs. (7)–(9) additionally quantify mean daily temperature and exposure duration above the 35 °C engineering reference. The passive-air case gives a daily mean temperature of 40.44 °C and remains above 35 °C for the entire prescribed 24-h period. By comparison, the reactive-liquid and predictive trajectories give daily mean temperatures of 30.84 and 29.44 °C, respectively, and remain below 35 °C throughout the simulated day.

The relative ordering is consistent with the general behavior reported for EV battery thermal-management systems: stronger active heat rejection can reduce both peak temperature and thermal nonuniformity, although it normally introduces additional hardware, auxiliary-energy demand, and control complexity [6, 10, 11, 24]. Predictive strategies can potentially improve this trade-off by acting before the most severe thermal load occurs rather than responding only after temperature has risen [20, 22, 23]. The present predictive trajectory, however, is a prescribed scenario and should not be interpreted as the measured response of a validated predictive controller.

The corresponding first-pack SoH trajectories are shown in Fig. 3. If each degradation relationship is propagated without replacement, the year-8 reference SoH values are 59.45% for passive air cooling, 73.79% for reactive liquid cooling, and 83.86% for predictive pre-cooling. These values describe the intrinsic strategy-specific degradation trajectories used to estimate battery service-life intervals; they do not represent the SoH of the actual in-service pack after a replacement has occurred.

Using Eq. (12), the first crossing of the 80% traction-battery EOL threshold occurs at 3.43 years for passive air cooling, 5.87 years for reactive liquid cooling, and 10.14 years for predictive pre-cooling. Consequently, predictive pre-cooling extends the modeled first-pack service interval by

$$10.14 - 3.43 = 6.71 \text{ years} \tag{34}$$

relative to passive air cooling, while reactive liquid cooling extends the interval by

$$5.87 - 3.43 = 2.44 \text{ years}. \tag{35}$$

These differences are important not only economically but also from a material-cycle perspective because they change when traction batteries enter replacement, second-life assessment, disassembly, or recycling pathways.

The annual replacement accounting further clarifies this effect. After the first passive-air battery reaches the EOL threshold, it is replaced in year 4 and its SoH clock is reset. Applying the same 3.43-year service interval to the replacement pack results in a second threshold crossing before the end of the eight-year study period, corresponding to a second replacement event in year 8. Reactive liquid cooling produces one replacement event in year 6, whereas predictive pre-cooling produces no replacement event within the eight-year horizon. Thus,

$$N_{\mathrm{EOL,pass}}(8) = 2, \qquad N_{\mathrm{EOL,react}}(8) = 1, \qquad N_{\mathrm{EOL,pred}}(8) = 0. \tag{36}$$

Relative to passive air cooling, reactive liquid cooling therefore defers one battery-pack EOL entry within the fixed study horizon, while predictive pre-cooling defers two. The term *defers* is important: these batteries will eventually require end-of-life management, and the present analysis does not imply avoided recycling or eliminated battery waste.

The relationship between temperature and lithium-ion battery aging is well established experimentally [12–15]. Nevertheless, the numerical SoH trajectories used here remain scenario assumptions. The coefficients k_s are not derived directly from the thermal trajectories or calibrated to a specific battery chemistry. Accordingly, the

results demonstrate the lifecycle consequences of alternative degradation scenarios rather than chemistry-specific battery-life predictions.

3.2 Replacement Events, Material-Cycle Implications, and Total Cost of Ownership

Figure 4 shows the eight-year TCO decomposition. Passive air cooling has the lowest initial hardware expenditure at USD 12,000 but the highest total modeled ownership cost because its shorter service interval produces two battery-replacement events and the highest downtime cost. The resulting eight-year TCO is USD 77,700 per vehicle.

Reactive liquid cooling increases initial hardware expenditure to USD 15,500 and also incurs the largest BTMS auxiliary-energy cost. However, its longer modeled battery service interval reduces the number of replacement events from two to one and decreases downtime. The resulting TCO is USD 72,500, representing

$$\frac{77{,}700 - 72{,}500}{77{,}700} \times 100 = 6.69\% \tag{37}$$

lower cost than the passive-air baseline.

Predictive pre-cooling has the highest initial hardware cost, USD 17,200, but does not require battery replacement within the eight-year horizon and has the lowest modeled downtime cost. Its total TCO is USD 62,000 per vehicle. The corresponding saving relative to passive air cooling is

$$\Delta C_{\text{pred}} = 77{,}700 - 62{,}000 = 15{,}700 \text{ USD}, \tag{38}$$

or

$$S_{\text{pred}} = \frac{15{,}700}{77{,}700} \times 100 = 20.21\%. \tag{39}$$

Relative to reactive liquid cooling, predictive pre-cooling reduces the eight-year TCO by USD 10,500, equivalent to 14.48%.

The cost decomposition explains why the lifecycle ranking differs from the capital-cost ranking. Relative to passive air cooling, predictive pre-cooling adds USD 5,200 in initial hardware cost, USD 2,000 in BTMS energy cost, and USD 800 in maintenance cost. These additional expenditures total USD 8,000. They are offset by USD 18,000 in avoided replacement expenditure within the eight-year horizon and USD 5,700 in reduced downtime, giving USD 23,700 in gross lifecycle benefit and a net saving of USD 15,700.

Importantly, the USD 18,000 replacement difference does not represent a single avoided replacement. In the revised event-based model it corresponds to two USD 9,000 replacement events in the passive-air case—one in year 4 and another in year 8—compared with no replacement event in the predictive case. This interpretation preserves the original eight-year TCO total while making the degradation, replacement, and material-cycle accounting internally consistent.

The same result can be interpreted from a material-cycle perspective. A shorter battery service interval increases the number of battery packs that must leave traction service during a fixed vehicle lifetime. In the present eight-year scenario, passive

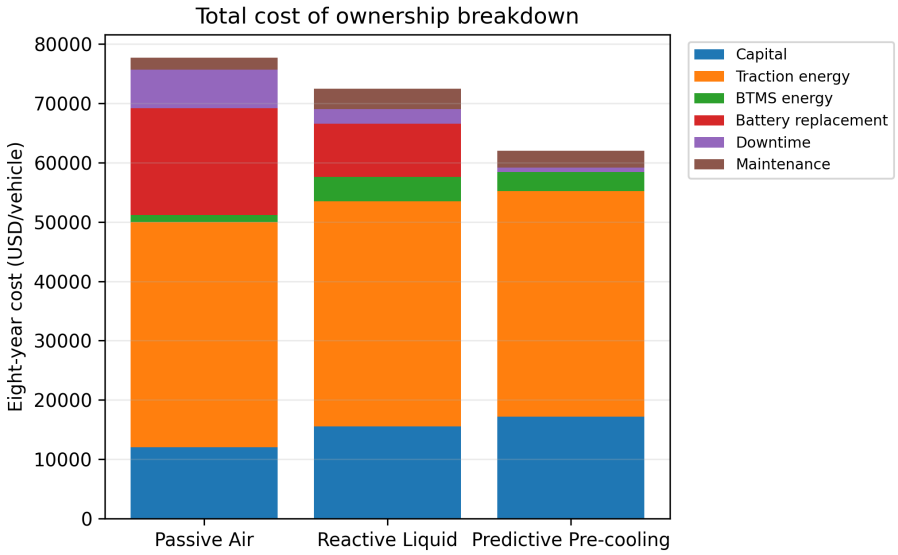


Fig. 4 Eight-year TCO decomposition for the three BTMS strategies.

air cooling produces two EOL-entry events per vehicle, reactive liquid cooling produces one, and predictive pre-cooling produces none. The predictive strategy therefore reduces the number of traction-battery retirement events occurring inside the study horizon by two per vehicle relative to passive cooling.

This finding should not be interpreted as a direct reduction in material waste. Battery mass, chemistry, second-life suitability, collection efficiency, recycling efficiency, and recovered-material yield are not modeled. Rather, the result describes an upstream service-life effect: improved thermal management can delay the timing at which battery packs enter downstream second-life and recycling systems. Such service-life extension is complementary to downstream circularity measures rather than a substitute for them [1, 3, 4].

3.3 Cumulative Cost and Break-Even Behavior

Figure 5 presents the cumulative ownership-cost trajectories calculated using Eq. (20). Excluding replacement events, the recurring annual expenditures are USD 5,962.5 for passive air cooling, USD 6,000 for reactive liquid cooling, and USD 5,600 for predictive pre-cooling.

Because predictive pre-cooling requires USD 5,200 more initial investment than passive air cooling, it begins the study with a cumulative-cost disadvantage. At the end of year 3,

$$C_{\mathrm{cum,pass}}(3) = 12{,}000 + 3(5{,}962.5) = 29{,}887.5 \text{ USD}, \tag{40}$$

while

$$C_{\text{cum,pred}}(3) = 17{,}200 + 3(5{,}600) = 34{,}000 \text{ USD}. \tag{41}$$

Hence,

$$D(3) = -4{,}112.5 \text{ USD}. \tag{42}$$

In year 4, the passive-air case incurs its first USD 9,000 battery-replacement charge. Its cumulative cost therefore becomes

$$C_{\text{cum,pass}}(4) = 12{,}000 + 4(5{,}962.5) + 9{,}000 = 44{,}850 \text{ USD}, \tag{43}$$

compared with

$$C_{\text{cum,pred}}(4) = 17{,}200 + 4(5{,}600) = 39{,}600 \text{ USD}. \tag{44}$$

The corresponding cost difference changes to

$$D(4) = 5{,}250 \text{ USD}. \tag{45}$$

Linear interpolation between the annual accounting points gives

$$y_{\text{BE}} = 3 + \frac{4112.5}{4112.5 + 5250} \approx 3.44 \text{ years}. \tag{46}$$

The value of 3.44 years should not be interpreted as a conventional continuously accruing financial payback period. The reversal occurs because the model applies a discrete battery-replacement event during year 4. Therefore, the more appropriate engineering interpretation is that predictive pre-cooling becomes economically favorable when the passive-air case reaches its first battery replacement interval.

The second passive-air replacement event occurs in year 8, ensuring that the cumulative passive cost reaches the same USD 77,700 total reported in the TCO decomposition. Reactive liquid cooling incurs one USD 9,000 replacement in year 6 and reaches USD 72,500 at year 8, whereas predictive pre-cooling reaches USD 62,000 without replacement.

These results reinforce the distinction between acquisition cost and lifecycle cost. A low-cost BTMS may remain economically attractive under mild conditions or short ownership periods, but its advantage can reverse when degradation causes one or more battery replacements to occur within the operating horizon. This mechanism is especially relevant to intensively utilized logistics fleets, where downtime and replacement events directly affect vehicle availability and resource turnover.

3.4 Sensitivity to Tropical Ambient Temperature and Electricity Tariff

The ambient-temperature sensitivity shown in Fig. 6 illustrates how the assumed economics become increasingly dependent on thermal stress as tropical conditions intensify. The passive-air screening relationship increases with $(T_a - 28)^{1.5}$, whereas the predictive relationship increases linearly with $T_a - 28$.

At 28 °C, the passive relationship gives USD 5,000/year compared with USD 6,200/year for predictive pre-cooling. Under relatively mild conditions, the simpler passive strategy is therefore favored in this sensitivity submodel. Solving

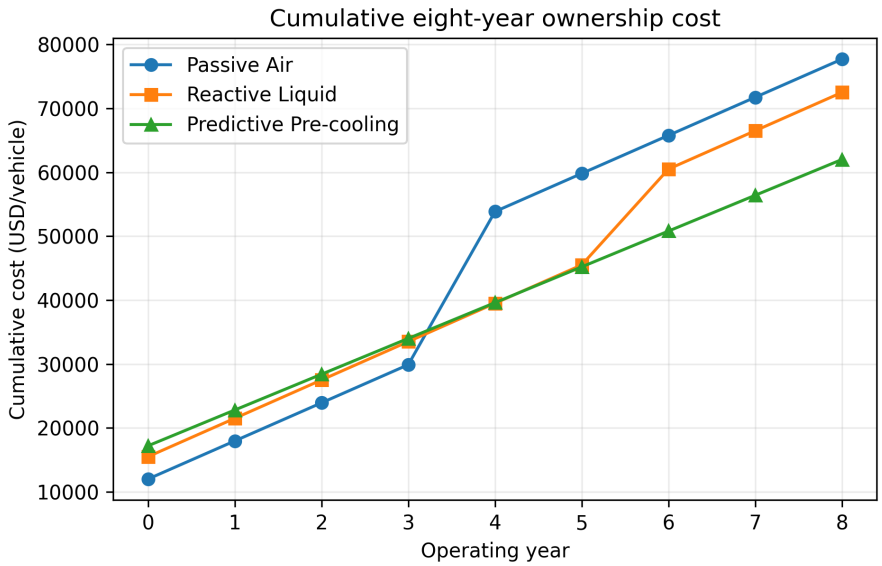


Fig. 5 Cumulative eight-year ownership cost. Passive-air battery replacements occur in years 4 and 8, while reactive liquid cooling requires one replacement in year 6.

$$5000 + 350(T_a - 28)^{1.5} = 6200 + 80(T_a - 28) \tag{47}$$

gives a crossover temperature of approximately 30.52 °C.

At 35 °C, the modeled values increase to approximately USD 11,482/year for passive air cooling and USD 6,760/year for predictive pre-cooling. At 42 °C, they become approximately USD 23,334/year and USD 7,320/year, respectively. The increasing separation is a direct consequence of the mathematical forms assigned to the two sensitivity curves and should therefore be interpreted as a scenario-screening result rather than an experimentally measured nonlinear cost response.

Nevertheless, the analysis illustrates an important design implication: the economic value assigned to improved thermal management becomes more pronounced as thermal exposure becomes more severe. This is particularly relevant to tropical logistics applications, where elevated ambient temperature can increase cooling demand, energy consumption, and degradation risk [15–18].

Electricity-price sensitivity produces a different trend. At the reference electricity tariff of USD 0.12/kWh, the combined traction and BTMS energy-cost terms are USD 39,200 for passive air cooling and USD 41,200 for predictive pre-cooling. The predictive strategy therefore carries a USD 2,000 energy-cost penalty because of its larger assumed BTMS auxiliary-energy requirement.

At USD 0.25/kWh, the corresponding energy-related costs rise to approximately USD 81,667 and USD 85,833, increasing the absolute energy-cost difference to approximately USD 4,167. Thus, higher electricity prices act against predictive pre-cooling in the energy submodel.

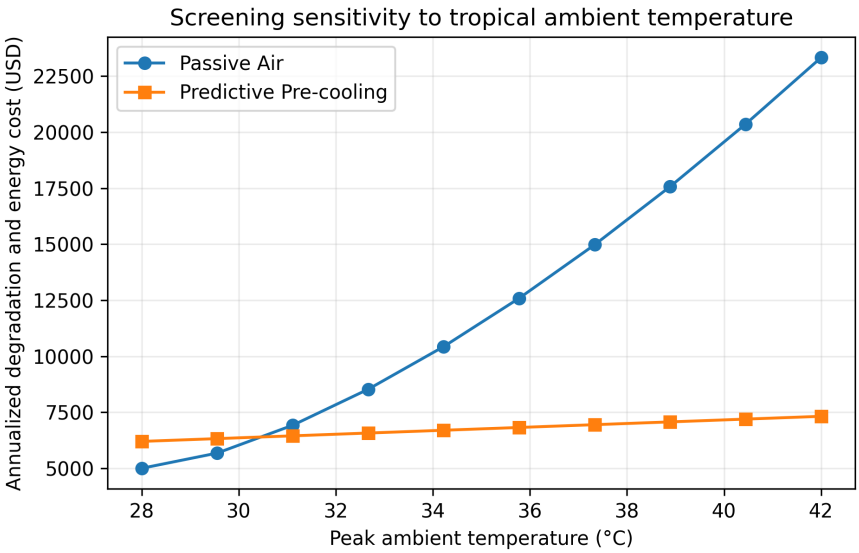


Fig. 6 Sensitivity of the prescribed degradation-and-energy cost indicator to peak ambient temperature.

However, this result does not reverse the overall TCO ranking within the investigated tariff range because the modeled replacement and downtime savings are larger than the additional energy expenditure. The predictive strategy is therefore not economically preferred because it consumes less electricity; it is preferred because the assumed service-life and availability benefits dominate the added thermal-management energy cost.

3.5 Predictive Pre-Cooling and Fleet-Scale Implications

Figure 8 illustrates the saturating pre-cooling relationship defined in Eq. (29). A 15-min pre-cooling period produces a modeled peak-temperature reduction of 5.37 °C, corresponding to 63.2% of the 8.5 °C asymptotic reduction. Extending pre-cooling to 30 min increases the reduction to 7.35 °C, or 86.5% of the asymptote, while 60 min gives 8.34 °C, approximately 98.2%.

The derivative in Eq. (30) quantifies the diminishing return. The initial marginal temperature benefit is approximately 0.567 °C/min, decreases to approximately 0.208 °C/min at 15 min, and falls to approximately 0.077 °C/min at 30 min. Consequently, most of the modeled thermal benefit is obtained within the first 30 min.

This diminishing-return behavior has practical importance for logistics operations. Excessive pre-cooling would continue to require auxiliary energy and depot dwell time while providing progressively smaller thermal benefit. A future predictive controller should therefore optimize pre-cooling duration against energy use, departure schedule, expected route load, ambient temperature, and battery degradation rather than maximizing cooling duration alone.

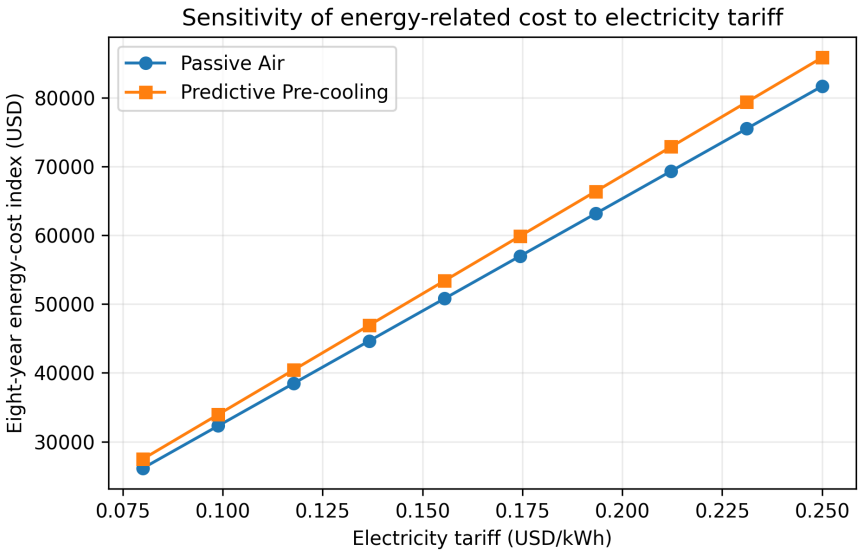


Fig. 7 Sensitivity of the eight-year energy-related cost component to electricity tariff.

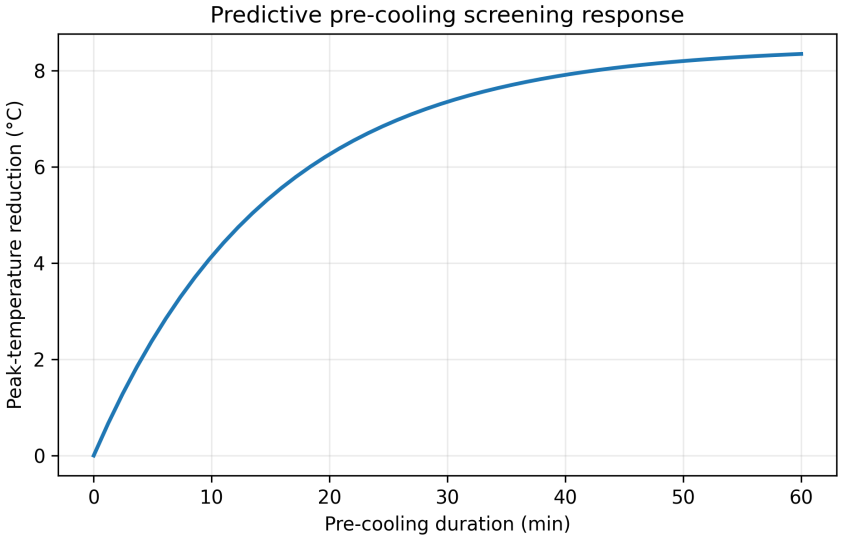


Fig. 8 Prescribed relationship between pre-cooling duration and peak-temperature reduction.

Fleet-scale extrapolation highlights the economic consequence of the per-vehicle result. The predictive strategy provides an eight-year undiscounted saving of USD 15,700 per vehicle relative to passive air cooling. Equation (31) therefore gives cumulative fleet savings of USD 0.157 million for 10 vehicles, USD 0.785 million for

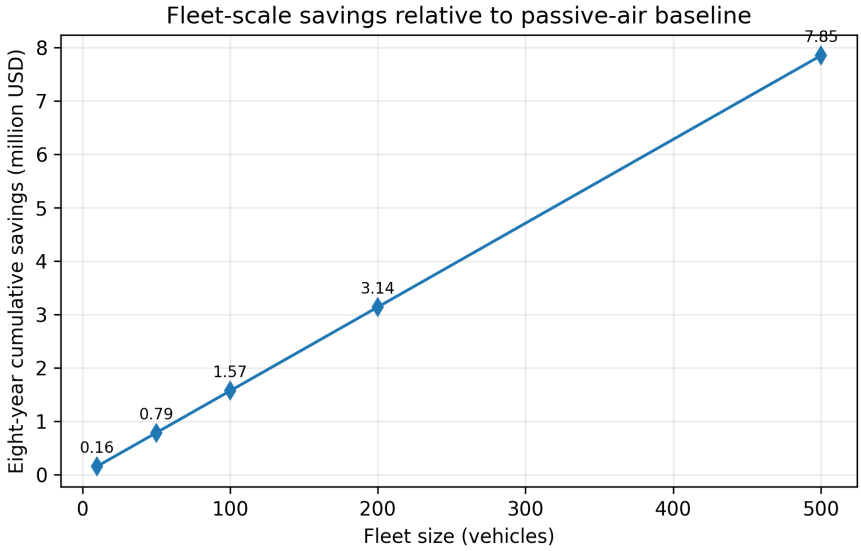


Fig. 9 Eight-year fleet-scale cumulative savings of predictive pre-cooling relative to passive air cooling.

50 vehicles, USD 1.57 million for 100 vehicles, USD 3.14 million for 200 vehicles, and USD 7.85 million for 500 vehicles.

The material-cycle implication scales in the same manner. Because passive air cooling produces two EOL-entry events per vehicle within the eight-year horizon while predictive pre-cooling produces none, the modeled number of EOL pack entries deferred beyond the study horizon is

$$N_{\text{deferred,pred}} = 2N. \tag{48}$$

Thus, the corresponding values are 20 packs for a 10-vehicle fleet, 100 packs for 50 vehicles, 200 packs for 100 vehicles, 400 packs for 200 vehicles, and 1,000 packs for 500 vehicles.

These values should be interpreted as service-life and timing indicators rather than waste-reduction quantities. No claim is made that these batteries permanently avoid end-of-life treatment. Instead, the analysis indicates how extending useful traction-battery life can reduce the number of packs entering the EOL management chain during a fixed operating horizon, thereby slowing material turnover and complementing downstream reuse and recycling strategies.

Table 3 summarizes the principal thermal, battery-life, material-cycle, and economic results.

4 Engineering and Material-Cycle Interpretation

The results reveal that BTMS selection is simultaneously a thermal, economic, and material-cycle decision. The passive-air scenario minimizes initial equipment cost and

Table 3 Summary of principal thermal, service-life, material-cycle, and economic indicators.

Strategy	Peak T_b (°C)	First-pack EOL (year)	Replacement events (8 years)	Deferred EOL entries vs. passive	TCO (USD)	Saving (%)
Passive air	51.07	3.43	2	–	77,700	–
Reactive liquid	33.41	5.87	1	1	72,500	6.69
Predictive pre-cooling	31.00	10.14	0	2	62,000	20.21

auxiliary-energy demand, but the imposed high-temperature exposure produces the shortest modeled battery service interval and the largest number of replacement events. By contrast, the predictive pre-cooling scenario requires greater initial investment and auxiliary energy but delays the 80% SoH threshold beyond the eight-year ownership horizon.

The first implication is that thermal-management performance should not be judged solely by peak temperature or cooling-energy consumption. Within the present scenarios, the economic value of active and predictive cooling arises primarily from the interaction between thermal exposure, battery service life, replacement expenditure, and vehicle availability. This explains why predictive pre-cooling has a higher energy-related cost than passive air cooling while still producing the lowest total ownership cost.

The second implication concerns battery material turnover. Every battery replacement introduces another traction battery into the vehicle system and moves the retired pack toward second-life evaluation, disassembly, or recycling. Extending battery service life can therefore delay the rate at which packs enter these downstream material-management pathways. In the present eight-year comparison, the passive-air case generates two EOL-entry events per vehicle, the reactive-liquid case one, and the predictive case none. The modeled benefit of thermal management is therefore not only lower replacement expenditure but also slower turnover of traction-battery assets.

This interpretation is consistent with the broader principle of waste prevention and service-life extension within sustainable material management [1]. It also complements, rather than replaces, downstream battery-recycling strategies [3, 4]. Even a long-lived battery eventually reaches retirement and requires appropriate second-life assessment or material recovery. Thermal management influences *when* that transition occurs; recycling determines *how* the retired material is subsequently managed.

The third implication is that the economic response is inherently nonlinear because replacement is a threshold-driven event. The SoH trajectory in Eq. (10) is continuous, but once the 80% threshold is crossed, a discrete USD 9,000 replacement expenditure is introduced. Small changes in degradation coefficient, EOL criterion, utilization, or ownership horizon can therefore move a major cost item into or outside the study period. Replacement timing is consequently one of the most influential assumptions in the analysis.

Finally, predictive operation is most attractive where future thermal load is sufficiently structured to support anticipatory action. Scheduled logistics fleets provide a plausible application because route departure, charging windows, depot dwell periods, and expected ambient conditions may be known in advance. The diminishing-return relationship in Eq. (30) indicates, however, that increasingly long pre-cooling periods

are not necessarily desirable. A practical controller would need to balance thermal benefit against auxiliary-energy consumption and operational constraints.

5 Limitations and Future Work

The numerical results should be interpreted within the scope of a deterministic screening study. The framework contains thermal, degradation, material-cycle, and economic layers, but the coupling among these layers is parametric rather than fully physics-based. The thermal trajectories are analytical surrogates rather than solutions of a validated electrothermal battery model, while the degradation coefficients are prescribed values rather than parameters identified for a specific lithium-ion chemistry.

The first-pack SoH curves are used to determine service-life intervals and are reset when replacement occurs in the ownership model. They should therefore not be interpreted as continuous eight-year histories of a single physical battery after replacement. Likewise, the 80% EOL criterion represents traction-service retirement only; it does not imply that the battery has reached absolute technical or material end of life.

The material-cycle analysis is limited to pack-level EOL-entry events. Battery mass, cathode chemistry, remaining useful capacity, second-life eligibility, disassembly yield, recycling recovery efficiency, recovered-material quality, and avoided primary-material production are not modeled. Consequently, the study does not quantify waste mass, recycling benefit, carbon footprint, or life-cycle environmental impact.

The TCO analysis is also simplified. Cash flows are undiscounted, recurring costs are distributed uniformly across the eight-year horizon, and replacement is treated as an annual discrete event. Financing, taxation, inflation, insurance, residual value, battery salvage value, charger infrastructure, stochastic electricity prices, and heterogeneous fleet utilization are outside the current system boundary.

Future work should therefore couple a validated electrothermal battery model with measured tropical logistics duty cycles and experimentally parameterized calendar- and cycle-aging relationships. Battery chemistry, pack mass, second-life suitability, and recycling pathways should subsequently be incorporated to convert EOL event counts into material-flow indicators. An expanded study could further integrate discounted cash flow, uncertainty propagation, life-cycle assessment, and material-flow analysis. Predictive pre-cooling should ultimately be implemented using a validated MPC or learning-based controller and tested using measured battery, route, charging, and ambient-temperature data.

6 Conclusion

This study developed a deterministic scenario-based framework for examining how EV battery thermal-management strategies can influence battery thermal exposure, service life, end-of-life (EOL) timing, replacement frequency, and lifecycle ownership cost under tropical logistics conditions. Three strategies—passive air cooling, reactive liquid cooling, and predictive pre-cooling—were evaluated under common ambient, utilization, energy, and eight-year ownership assumptions. The prescribed peak-day scenarios produced maximum battery temperatures of 51.07, 33.41, and 31.00 °C, with corresponding daily mean temperatures of 40.44, 30.84, and 29.44 °C, respectively.

Within the paired degradation scenarios, the first-pack 80%-SoH threshold was reached after 3.43 years for passive air cooling, 5.87 years for reactive liquid cooling, and 10.14 years for predictive pre-cooling. These results indicate that improved thermal control can substantially extend the modeled traction-battery service interval under hot-climate operation.

When the service-life intervals were propagated into the eight-year replacement model, passive air cooling produced two battery-replacement events, reactive liquid cooling produced one, and predictive pre-cooling produced none within the study horizon. The corresponding total costs of ownership were USD 77,700, USD 72,500, and USD 62,000 per vehicle. Predictive pre-cooling therefore reduced the modeled TCO by USD 15,700, or 20.21%, relative to passive air cooling. The economic advantage arose primarily from avoiding two USD 9,000 battery-replacement events and reducing modeled downtime, which more than compensated for the higher initial hardware, auxiliary-energy, and maintenance costs. The cumulative-cost comparison further showed that the economic ranking changes during the first passive-battery replacement interval in year 4, with an indicative interpolated crossover of approximately 3.44 years.

The results also provide a material-cycle interpretation that extends beyond conventional BTMS cost comparison. Over the fixed eight-year horizon, reactive liquid cooling defers one traction-battery EOL entry per vehicle relative to passive air cooling, while predictive pre-cooling defers two. At fleet scale, this corresponds to 1,000 deferred EOL pack entries for a 500-vehicle predictive scenario relative to the passive baseline. These values should be interpreted as service-life and timing indicators rather than as avoided waste or avoided recycling, because downstream second-life suitability, battery mass, chemistry, disassembly, recycling efficiency, and recovered-material flows were not modeled. Nevertheless, the analysis demonstrates that extending battery service life through improved thermal management can slow the rate at which traction batteries enter downstream EOL management systems and can therefore complement reuse and recycling strategies.

The principal implication is that BTMS selection for high-utilization EV fleets should be assessed using an integrated lifecycle perspective rather than by cooling performance, auxiliary-energy consumption, or acquisition cost alone. Under the present scenarios, the preferred strategy emerges from the combined effects of thermal exposure, degradation, replacement timing, vehicle availability, and ownership cost. The sensitivity results further indicate that ambient temperature, electricity tariff, and pre-cooling duration can materially influence the relative attractiveness of competing strategies, particularly under hot-climate operation.

The present findings remain scenario-based and should not be interpreted as experimentally validated battery-life, waste-reduction, or investment forecasts. Future work should couple validated electrothermal models with chemistry-specific calendar- and cycle-aging relationships, measured tropical logistics duty cycles, and experimentally verified predictive control. Extending the framework to battery mass and chemistry, second-life eligibility, recycling pathways and recovery yields, discounted

cash-flow analysis, life-cycle assessment, material-flow analysis, and uncertainty propagation would enable a more complete evaluation of the economic and circular-material consequences of EV battery thermal management.

Statements and Declarations

Funding. Funding information should be confirmed by all authors before submission.

Competing Interests. The competing-interest statement should be confirmed by all authors before submission.

Author Contributions. P.Ph. and P.Pr. contributed to the study concept, scenario definition, and techno-economic analysis. S.S. contributed to methodology development, engineering interpretation, and critical manuscript revision. T.K. contributed to technical review and manuscript development. W.R. contributed to project coordination, interpretation of the logistics application, and manuscript review. All authors should confirm the final contribution statement before submission.

Data Availability. The numerical inputs and deterministic scenario equations used to generate the reported results are contained in the manuscript and accompanying analysis files. Any additional supporting data should be confirmed by the authors before submission.

Code Availability. The Python analysis script used to generate the figures and summary tables is included in the submission package for reproducibility of the scenario calculations.

Ethics, Consent to Participate, and Consent to Publish declarations. Not applicable.

References

[1] Sakai, S.-i., Yano, J., Hirai, Y., Asari, M., Yanagawa, R., Matsuda, T., Yoshida, H., Yamada, T., Kajiwara, N., Suzuki, G., Kunisue, T., Takahashi, S., Tomoda, K., Wuttke, J., Mählitz, P., Rotter, V.S., Grosso, M., Astrup, T.F., Cleary, J., Oh, G.-J., Liu, L., Li, J., Ma, H.-w., Chi, N.K., Moore, S.: Waste prevention for sustainable resource and waste management. J Mater Cycles Waste Manag **19**, 1295–1313 (2017) https://doi.org/10.1007/s10163-017-0586-4

[2] Karagoz, S., Aydin, N., Simic, V.: End-of-life vehicle management: a comprehensive review. J Mater Cycles Waste Manag **22**, 416–442 (2020) https://doi.org/10.1007/s10163-019-00945-y

[3] Pigłowska, M., Kurc, B., Fuć, P., Szymlet, N.: Novel recycling technologies and safety aspects of lithium ion batteries for electric vehicles. J Mater Cycles Waste Manag **26**, 2656–2669 (2024) https://doi.org/10.1007/s10163-024-02028-z

[4] Bräunig, G., Hertel, D., Thürer, M.: Towards recycling excellence: a systematic review of applied lean methods within the disassembly of electric vehicle battery systems. J Mater Cycles Waste Manag **27**, 4127–4142 (2025) https://doi.org/10.1007/s10163-025-02368-4

[5] Bernardi, D., Pawlikowski, E., Newman, J.: A general energy balance for battery systems. J Electrochem Soc **132**(1), 5–12 (1985) https://doi.org/10.1149/1.2113792

[6] Maiorino, A., Cilenti, C., Petruzziello, F., Aprea, C.: A review on thermal management of battery packs for electric vehicles. Appl Therm Eng **238**, 122035 (2024) https://doi.org/10.1016/j.applthermaleng.2023.122035

[7] El Kassar, R., Al Takash, A., Faraj, J., Hammoud, M., Khaled, M., Ramadan, H.S.: Recent advances in lithium-ion battery integration with thermal management systems for electric vehicles: A summary review. J Energy Storage **91**, 112061 (2024) https://doi.org/10.1016/j.est.2024.112061

[8] Khan, A., Yaqub, S., Ali, M., Ahmad, A.W., Nazir, H., Khalid, H.A., Iqbal, N., Said, Z., Sopian, K.: A state-of-the-art review on heating and cooling of lithium-ion batteries for electric vehicles. J Energy Storage **76**, 109852 (2024) https://doi.org/10.1016/j.est.2023.109852

[9] Chavan, S., Venkateswarlu, B., Salman, M., Liu, J., Pawar, P., Joo, S.W., Choi, G.S., Kim, S.C.: Thermal management strategies for lithium-ion batteries in electric vehicles: Fundamentals, recent advances, thermal models, and cooling techniques. Int J Heat Mass Transf **232**, 125918 (2024) https://doi.org/10.1016/j.ijheatmasstransfer.2024.125918

[10] Hwang, F.S., Confrey, T., Reidy, C., Picovici, D., Callaghan, D., Culliton, D., Nolan, C.: Review of battery thermal management systems in electric vehicles. Renew Sustain Energy Rev **192**, 114171 (2024) https://doi.org/10.1016/j.rser.2023.114171

[11] Gharehghani, A., Rabiei, M., Mehranfar, S., Saeedipour, S., Mahmoudzadeh Andwari, A., García, A., Reche, C.M.: Progress in battery thermal management systems technologies for electric vehicles. Renew Sustain Energy Rev **202**, 114654 (2024) https://doi.org/10.1016/j.rser.2024.114654

[12] Maures, M., Zhang, Y., Martin, C., Delétage, J.-Y., Vinassa, J.-M., Briat, O.: Impact of temperature on calendar ageing of lithium-ion battery using incremental capacity analysis. Microelectron Reliab **100–101**, 113364 (2019) https://doi.org/10.1016/j.microrel.2019.06.056

[13] Saldaña, G., San Martín, J.I., Zamora, I., Asensio, F.J., Oñederra, O., González-Pérez, M.: Empirical calendar ageing model for electric vehicles and energy storage systems batteries. J Energy Storage **55**, 105676 (2022) https://doi.org/

10.1016/j.est.2022.105676

[14] Bamdezh, M.A., Molaeimanesh, G.R.: Aging behavior of an electric vehicle battery system considering real drive conditions. Energy Convers Manag **304**, 118213 (2024) https://doi.org/10.1016/j.enconman.2024.118213

[15] Bamdezh, M., Molaeimanesh, G.R., Mohammadi Saman Kand, R., Mostajeran, M.: Effects of temperate, cold, and warm climate conditions on electric vehicle and battery thermal management system performance: Energy usage, battery aging, and carbon footprints. Energy Convers Manag **339**, 119935 (2025) https://doi.org/10.1016/j.enconman.2025.119935

[16] Parker, N.C., Kuby, M., Liu, J., Stechel, E.B.: Extreme heat effects on electric vehicle energy consumption and driving range. Appl Energy **380**, 125051 (2025) https://doi.org/10.1016/j.apenergy.2024.125051

[17] Lotchouang Fuste, H., Kibong Tony, M., Nyatte, S., Sapnken, F.E., Mewoli, A.E., Tamba, J.G.: Experimental characterization of electric vehicle battery degradation in tropical environments: Influence of climatic factors and local driving conditions. Energy Reports **15**, 109126 (2026) https://doi.org/10.1016/j.egyr.2026.109126

[18] Fatmawati, U.D., Garniwa, I., Husnayain, F.: Mitigating ev battery degradation risks driven by high ambient temperatures in tropical climates: A theoretical review and data-driven analysis of public charging stations. J Energy Storage **172**, 122906 (2026) https://doi.org/10.1016/j.est.2026.122906

[19] Ma, Y., Ding, H., Mou, H., Gao, J.: Battery thermal management strategy for electric vehicles based on nonlinear model predictive control. Measurement **186**, 110115 (2021) https://doi.org/10.1016/j.measurement.2021.110115

[20] Wang, W., Ren, J., Yin, X., Qiao, Y., Cao, F.: Energy-efficient operation of the thermal management system in electric vehicles via integrated model predictive control. J Power Sources **603**, 234415 (2024) https://doi.org/10.1016/j.jpowsour.2024.234415

[21] Wu, Y., Huang, Z., Li, D., Li, H., Peng, J., Stroe, D., Song, Z.: Optimal battery thermal management for electric vehicles with battery degradation minimization. Appl Energy **353**, 122090 (2024) https://doi.org/10.1016/j.apenergy.2023.122090

[22] Ma, Y., Ma, Q., Liu, Y., Gao, J., Chen, H.: Two-level optimization strategy for vehicle speed and battery thermal management in connected and automated EVs. Appl Energy **361**, 122928 (2024) https://doi.org/10.1016/j.apenergy.2024.122928

[23] Tomanik, V., Bares, P., Aronis, A.N., Pla, B.: Integrated predictive control of

battery thermal management in electric vehicles during driving and fast charging. Appl Therm Eng **289**, 129711 (2026) https://doi.org/10.1016/j.applthermaleng.2026.129711

[24] Rawat, S.S., Kumar, R.: Techno-economic analysis of cooling technologies used in electric vehicle battery thermal management: A review. J Energy Storage **103**, 114135 (2024) https://doi.org/10.1016/j.est.2024.114135

[25] Park, S.-W., Son, S.-Y.: Techno-economic analysis for the electric vehicle battery aging management of charge point operator. Energy **280**, 128095 (2023) https://doi.org/10.1016/j.energy.2023.128095

[26] Suttakul, P., Wongsapai, W., Fongsamootr, T., Mona, Y., Poolsawat, K.: Total cost of ownership of internal combustion engine and electric vehicles: A real-world comparison for the case of thailand. Energy Rep **8**, 545–553 (2022) https://doi.org/10.1016/j.egyr.2022.05.213